Journal of Statistical Physics, Vol. 61, Nos. 3/4, 1990

Universal Multifractal Properties of Circle Maps from the Point of View of Critical Phenomena. I. Phenomenology

B. Fourcade[1,2,3] and A.-M. S. Tremblay[1]

Received June 14, 1989; final June 11, 1990

The strange attractor for maps of the circle at criticality has been shown to be characterized by a remarkable infinite set of exponents. This characterization by an infinite set of exponents has become known as the "multifractal" approach. The present paper reformulates the multifractal properties of the strange attractor in a way more akin to critical phenomena. This new approach allows one to study the universal properties of both the critical point and of its vicinity within the same framework, and it allows universal properties to be extracted from experimental data in a straightforward manner. Obtaining Feigenbaum's scaling function from the experimental data is, by contrast, much more difficult. In addition to the infinite set of exponents, universal amplitude ratios here appear naturally. To study the crossover region near criticality, a "correlation time," which plays a role analogous to the "correlation length" in critical phenomena, is introduced. This new approach is based on the introduction of a joint probability distribution for the positive integer moments of the closest-return distances. This joint probability distribution is physically motivated by the large fluctuations of the multifractal moments with respect to the choice of origin. The joint probability distribution has scaling properties analogous to those of the free energy close to a critical point.

KEY WORDS: Onset of chaos; circle map; quasiperiodic route to chaos; multifractals; infinite set of exponents; critical phenomena; universality.

1. INTRODUCTION

Strange attractors which appear on the borderline of chaos are now experimentally accessible objects[1] which have universal scaling properties.

[1] Département de Physique et Centre de Recherche en Physique du Solide, Université de Sherbrooke, Sherbrooke, Québec, Canada, J1K 2R1.

[2] Present address: Department of Physics, Simon Fraser University, Burnaby British Columbia, Canada, V5A 156.

[3] Present address: Institut von Laue. Paul Langevin, B.P. 156X, Grenoble Cedex, 38042, France.

0022-4715/90/1100-0607$06.00/0

These properties are understood through renormalization group concepts.[2] At criticality, there are two ways to emphasize universal properties. First, there are quantities such as Feigenbaum's scaling function, which characterizes locally the strange attractor. However, as underlined in ref. 3, since Feigenbaum's scaling function is everywhere discontinuous, its measurement is very sensitive to noise. By contrast to this local approach, there is a global way to look at the problem by averaging quantities along a trajectory. This is the multifractal approach, which, by contrast to the previous one, concentrates on smooth functions, namely on a continuous infinite set of exponents.

The traditional approach to scaling is based instead on the paradigm of critical phenomena. In this context also, scaling is understood through renormalization group concepts. However, the set of exponents is discrete, and, in general, only a few are experimentally accessible (For exceptions, see, for example, ref. 4.) Universal properties, on the other hand, are numerous. There are not only universal exponents, but also universal amplitude ratios and crossover functions.

The multifractal approach and critical phenomena have, up to now, been considered as quite different,[5] even though the multifractal problem is often cast in the language of a "thermodynamic formalism."[5] In the present paper, we wish to show how to obtain the universal multifractal properties of the strange attractors through a formalism which is as close as possible to the formalism of critical phenomena, and different from, but related to, the standard thermodynamic formalism. In particular, quantities leading to the exponents $\tau(q)$ play a role in our approach, but only the positive integer values of q are shown to be of interest. Furthermore, the Legendre transform of the $\tau(q)$, the $f(\alpha)$ function,[5] does not play any special role.

There are other physical systems where the multifractal approach has been extensively used (see ref. 6 for a review). A typical list includes, for example, percolation, localization, and diffusion-limited aggregation. In the context of percolation, we have discussed extensively the analogies between the multifractal character and the critical phenomena approach.[7] We believe that looking at multifractal properties for the circle map from the point of view of critical phenomena not only provides a framework which is unified, but also one which is very natural from the point of view of experimental measurements. Furthermore, the same approach is useful not only at the critical point, but also in its vicinity, in other words, it allows one to study universal crossover behavior.

In drawing analogies with critical phenomena and establishing the appropriate framework (see ref. 8; see ref. 9 for early versions of this work), we answer the following questions: (i) Do we need a *continuous* set of

exponents to characterize the critical properties of maps of the circle? (ii) How does the usual multifractal characterization depend on the starting point of the iteration? (iii) How can universal properties of the trajectory be accessed other than through multifractal exponents or through Feigenbaum's scaling function? In standard critical phenomena, it is known that in addition to exponents, universal ratios also characterize criticality and it would be useful to compute the corresponding quantities in the context of dynamical systems. (iv) How can the crossover from the critical region be characterized in the multifractal framework? Our approach should provide useful methods to characterize universal quantities in the neighborhood of the critical point.

The following, then, shows that the multifractal structure of strange attractors for quasiperiodic systems involves universal quantities analogous to universal scaling functions in critical phenomena. These functions are characteristic of the fixed point of the functional renormalization group for maps of the circle with a cubic inflection point,[2] so that this approach is sufficiently general to consider, from a unified point of view, the system at criticality and in the crossover region. Under iterations, at criticality, of one point chosen at random, the universal properties of the trajectory can be characterized by a universal probability distribution which plays a role analogous to the singular part of the free energy in thermodynamic critical phenomena. This probability distribution is the joint probability distribution for the positive integer moments of the closest-return distances. Renormalization group arguments[10] and proofs of some properties, such as the fact that the sample probability distribution for the starting point is not relevant, are detailed in a companion paper, which will be refered as II. The approach of the present paper (I) is descriptive. It should clarify both the analogies with critical phenomena and the data analysis most appropriate to these analogies.

The following section recalls the multifractal properties of maps of the circle and sets the notations. Section 3 discusses the variables which allow one to make connection with critical phenomena. Subsequently, Section 4 describes the fluctuations of the multifractal "moments" with respect to the starting point of the series: It is shown that at the critical point, these fluctuations can be characterized by nontrivial functions whose nonstrous fluctuations with respect to the starting point of the series lead one to adopt a probabilistic point of view by choosing the starting point as random. These fluctuations are demonstrated to be independent of the time scale at which the system is probed. In Section 5.1 a joint probability distribution for the moments of the closest-return distances is proposed to characterize the multifractal properties. This joint probability distribution is independent of the probability distribution of the starting point, is universal,

and contains all the hierarchy of critical exponents. In Section 5.2 the neighborhood of the critical region is considered by defining the analog of a correlation length. As the control parameters, defined in Section 2, are varied to approach the critical point along the two eigendirections of the renormalization group, this unique "correlation time" controls the fluctuations of all multifractal moments, irrespective of their order. The results of Section 5.1 are thus generalized to include the crossover to the subcritical region. In the conclusion, Section 6, the preceding results are discussed in connection with other work, and suggestions for extensions are given.

2. KNOWN PROPERTIES OF MAPS OF THE CIRCLE; NOTATION AND MOTIVATION

A general approach in dynamical systems consists in studying motion in phase space by means of maps instead of nonlinear differential equations. Quasiperiodic systems refer generically to systems where resonance effects between two nonlinearly coupled oscillators play a fundamental role in driving the system to a chaotic regime.[10] In the limit of an infinite dissipation and in the nonchaotic regime, the motion in phase space is concentrated on a two-dimensional torus. By taking the Poincaré section, the system can be analyzed by maps of the circle onto itself. An example, due to Arnold, of such a map is

$$\theta_{i+1} = f(\theta_i) \equiv \theta_i + \Omega - \frac{K}{2\pi} \sin(2\pi\theta_i) \tag{1a}$$

where for a general map of the circle, $f(\theta_i + 1) = f(\theta_i) + 1$, and where Ω and K will be called control parameters: Ω is the bare winding number and corresponds to the ratio of two frequencies, while K sets the level of nonlinearity. Alternatively, the mean winding number ρ (or the period P) and K can thus also be chosen as characteristic parameters of the dynamics. However, in this case, one point of the orbit has to be specified to uniquely define this orbit, since ρ and K correspond to a locking interval for Ω (ref. 11; for a discussion on the locking intervals, see ref. 12).

The hypothesis is that Eq. (1) represents the dynamics of the system, the trajectory in phase space being characterized by the successive iterates of a starting point. For a mean rotation number ρ [$\rho \equiv \lim_{n \to \infty} (\theta_{i+n} - \theta_i)/n$], taken as a rational number, the trajectory is periodic. Otherwise, when ρ is irrational, the successive iterates cover the circle in a dense way and P is infinite.

In the quasiperiodic framework, the appearance of a chatotic regime is concomitant with the loss of invertibility of Eq. (1) (or an equivalent map).

Referring the reader to a general reference for this point,[11] we now recall the main properties of maps of the circle at the critical point corresponding to a mean rotation number equal to the golden mean $[\sigma = (\sqrt{5}-1)/2]$.

Consider the suncritical region for maps such as Eq. (1). This is defined as the region of the parameter space where periodic orbits of rational period P exist for finite nonoverlapping intervals of Ω (locking intervals). As K is varied, these locking intervals sweep a set with Cantor-like structures which are usually referred to as Arnold tongues. As the control parameters are set to a critical value, the system is just on the borderline where overlapping between the different locking intervals can take place. In the mathematical literature this line is referred to as the critical line and corresponds to the line $K=1$ in Fig. 1. For the map of Eq. (1a), the critical bare winding number which corresponds to a golden-mean winding number (rotation number) is $\Omega_c(1) = 0.606661063569....$

Universal properties of maps of the circle with a cubic inflection point are described by the functional renormalization group of Feigenbaum *et al.*

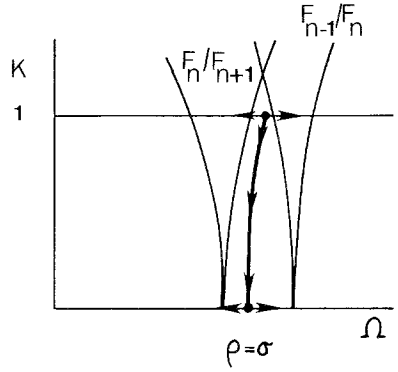

Fig. 1. Schematic "phase diagram" for the map (1a) in the space of parameters Ω and K. The arrowed lines correspond to the two unstable eigendirections of the renormalization group analysis. The thick curve corresponds to an irrational winding number σ. Under iteration of the renormalization group, this line is invariant. It joins the unstable fixed point describing the transition to chaos on the line $K=1$ to the trivial pure rotation fixed point at $K=0$. By analogy with critical phenomena, we refer to this line as the "discontinuity line." Two "Arnold tongues" corresponding to mean winding numbers F_n/F_{n+1} and F_{n-1}/F_n are also schematically indicated. For K equal to its critical value ($K=1$), the system is "phase locked" for the open interval of Ω contained between the edges of the tongue ($K=1$). Under iterations of the renormalization group, one flows away from the unstable fixed point while jumping alternatively across the discontinuity line from one tongue at a rational approximant of the golden mean to another. When this "phase diagram" is expressed as a function of the variables P (period or mean winding number) and K instead of Ω and K, the statistical description given by Eq. (13) becomes more natural.

and of Rand *et al.*[2] Hereafter, we shall refer to the latter formulation of the problem. Universality here means that the properties apply to a wide class of maps of the circle with a cubic inflection point at criticality. For example, we use in the sequel the map defined by

$$\theta_{i+1} = \theta_i + \Omega - K/2\pi[\sin(2\pi\theta_i) + 0.2\sin(6\pi\theta_i)] \tag{1b}$$

where the critical behavior for a rotation number equal to the golden mean is obtained for $\Omega = 0.60972055339196...$, $K = 0.625$. The map (1b) has a "phase diagram" similar to the one we just recalled for Eq. (1a).

As usual, the renormalization group equations can be viewed as a mapping in parameter space and, restricting ourselves to the (Ω, K) plane, the two unstable eigendirections are (i) the line $K = K_c$ and (ii) in the subcritical region, a curve $\Omega = \Omega_c(K)$ corresponding to a mean rotation number equal to[2] σ. On the line $K = K_c$, there is an open interval for Ω corresponding to a rational mean winding number. In that case the trajectory is periodic.[11] By analogy with phase transitions, the line $\Omega = \Omega_c(K)$ which, under renormalization, flows to a trivial fixed point (a pure irrational rotation with $K = 0$) will hereafter be referred to as the discontinuity line. As the renormalization group transformation is iterated in parameter space, one jumps alternatively across this line from one Arnold tongue to another.[2] These regions of the Ω–K plane give the periodic orbits whose successive periods are the series of the rational approximations for an irrational mean winding number. In the case of the golden mean, the Fibonacci series defined by

$$F_0 = 0; \qquad F_1 = 1; \qquad F_n = F_{n-1} + F_{n-2} \tag{2}$$

give the rational approximants, since

$$\sigma F_n = F_{n-1} - (-\sigma)^n; \qquad \sigma = \lim_{n \to \infty} \frac{F_{n-1}}{F_n} \tag{3}$$

At criticality, where ρ is irrational, the renormalization group equations show that the trajectory possesses universal scaling properties. These properties were first studied for the scaling of the distance between the origin and its closest iterate[2] as a function of the number of iterations. At the golden-mean winding number, the closest iterate changes every time the map is iterated a number of times which is equal to a Fibonacci number (see ref. 13 for a discussion of this point). The Fibonacci numbers then set the closest-return iterates, and they also approximate the golden mean, and hence they are a natural clock for these closest-return distances along the trajectory. To emphasize these properties, the same analysis was applied

by Halsey *et al.*[5] to all distances between one point and its iterates at successive Fibonacci time scales. Reference 1 shows that these are characterized by the scaling behavior

$$\sum_{1 \leqslant i \leqslant F_{n+1}} |\hat{f}^{(F_n)}(x_i) - x_i|^q \approx A_q F_{n+1}^{-\tau(q)} \tag{4}$$

where $\approx$ stands for "is asymptotically equal to," A_q is an amplitude which depends weakly on q (it is set equal to unity in ref. 5), and where $\tau(q)$ is a nonlinear function of q. From now on, the caret sign denotes the function modulo one. Note that, by definition, $\hat{f}^{(F_n)}(x) \equiv f^{(F_n)}(x) - F_{n-1}$. Also, x_i labels the $(i-1)$th iterate of x_1,

$$x_i \equiv f^{(i-1)}(x_1); \qquad f^{(i)} = f \circ f \circ f \circ f \cdots \circ f; \quad i \text{ times} \tag{5}$$

and the starting point of the series x_1 is taken as the origin, where the cubic inflection point is located. $|\hat{f}^{(F_n)}(x_i) - x_i|$ is a distance, and for F_n a Fibonacci number, it is the smallest distance between x_i and one of its iterates up to F_n. Hence the name "closest-return distances." The expression (4) will be called a multifractal "moment," for reasons which will appear more clearly in the next section.

To motivate definition (4) a bit more, consider an F_{n+1} periodic orbit. As suggested by (4), draw an arc between the first point and its F_nth iterate, repeating the procedure for the first F_{n+1} iterates. The set of arcs then covers the circle without overlap (Fig. 2a). When the mean winding number is irrational, the same procedure can be applied with an arbitrary F_n, but, in that case, there always exist small gaps in the covering (Fig. 2b). Note that when one varies the pure rotation number on a locking interval which is on the critical line $K=1$, the closest-return distances of the finite series of points are changed, and this change is nonuniform along the trajectory (Fig. 2c). On the line $\Omega = \Omega_c(K)$, on the other hand, corresponding to an irrational winding number, the starting point of the series should be arbitrary because there is no periodic point (stable or unstable).

In the work of Halsey *et al.*,[5] the properties of (4) were studied only at the critical point $\Omega = \Omega_c(1)$, and, furthermore, the starting point of the series was always taken as the origin defined above. We will see in what follows that when the starting point x_1 is not the origin, the amplitudes in Eq. (4) become functions $A_q(F_n, x_1)$ of the starting point x_1 and of the time scale F_n, which are highly irregular but of bounded variation. While the scaling properties of the multifractal moments are given by the envelope $F_{n+1}^{-\tau(q)}$, interesting universal properties are also hidden in these amplitudes. The characterization of these universal properties is a strong motivation for the present work.

The Legendre transform of the function $\tau(q)$, the so-called $f(\alpha)$ function, does not play any special role in our analysis: Since the Legendre transform is an involution, knowledge of either function completely specifies the other. For the sake of completeness, however, the $f(\alpha)$ function is introduced in the Appendix from a point of view closer in spirit to our approach.

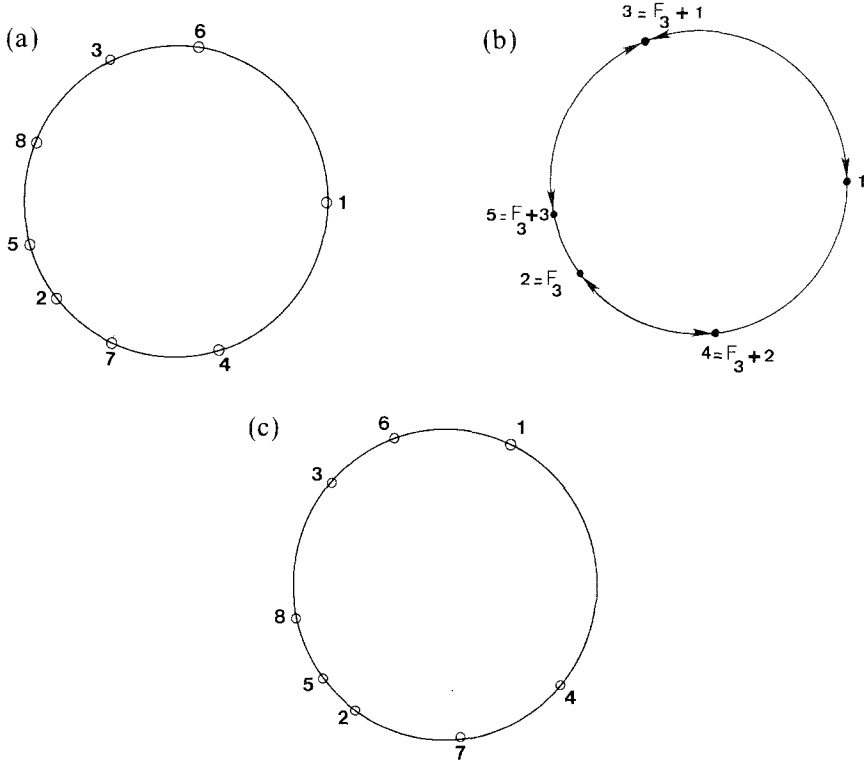

Fig. 2. Geometrical illustration of the distances entering the definition (10) of the multifractal moments for the periodic and the irrational cases. (a) The first 8 iterates of the origin for the map (1a) when the system is periodic with a period $F_6 = 8$. Note that the set of arcs between an iterate and the following $F_5 = 5$th one covers the circle without overlaps. Note that the arc between the 4th one covers the circle without overlaps. Note that the arc between the 4th iterate and the 9th one, for example, is between the 4th and the first iterate [9 Mod(8)]. (b) The first four iterates of the origin when the control parameters are at their critical value for the golden-mean winding number. In this case, $F_n = 2$ in Eq. (10), the closest-return distances are between a point and the second iterate that follows. Only the arcs with arrows are taken into account by the definition (10). The whole circle is not covered by these arcs. (c) Same as (a), except that the starting point is not the origin (The corresponding bare winding number Ω is different). The circles (c) and (a) cannot be superposed by only a global rotation.

3. THE POSITIVE INTEGER MOMENTS CHARACTERIZE COMPLETELY THE DISTRIBUTION OF THE CLOSEST-RETURN DISTANCES

As mentioned in the introduction, multifractality is not a property which manifests itself only in the case of dynamical systems. For percolating networks, the positive integer moments of the current distribution are the ones which are accessible through electrical noise measurements.[14] In a manner analogous to that used for the corresponding quantities in the percolation case,[7] let us introduce the distribution of closest-return distances $\mathbb{P}(x_1, l)$, whose moments are proportional to Eq. (4):

$$\mathbb{P}(x_1, l) = \frac{1}{F_{n+1}} \sum_{1 \leqslant i \leqslant F_{n+1}} \delta(l - |\hat{f}^{(F_n)}(x_i) - x_i|) \tag{6}$$

The positive integer moments suffice to characterize completely the distribution $\mathbb{P}$ of Eq. (6). This follows directly from the Bernstein–Hausdorff reconstruction theorem[15] of probability theory because the closest-return distances l are concentrated on a finite interval. In the present case, we normalize the circle to unity so that l is in the interval $]0, 1]$. This theorem can also be proved for the case of delta function distributions such as (6). The more precise statement of convergence is that the distribution $\mathbb{P}_N(x_1, l)$ obtained from the N first integer moments by (the double bar refers to quantities averaged with respect to the original distribution $\mathbb{P}$)

$$\mathbb{P}_N(x_1, l) = \sum_{k=0}^{N} \frac{N!}{k!\,(N-k)!} \overline{\overline{l^k (1-l)^{N-k}}}\, \delta\left(l - \frac{k}{N}\right) \tag{7}$$

converges to the original probability distribution. This convergence is defined in the sense of distributions, namely,

$$\lim_{N \to \infty} \int_0^1 dl\, \mathbb{P}_N(x_1, l) \mathscr{f}(l) = \int_0^1 dl\, \mathbb{P}(x_1, l) \mathscr{f}(l) \tag{8}$$

where $\mathscr{f}$ is a continuous function, and where the right-hand side is assumed to exist [Eq. (4) corresponds to the choice $\mathscr{f}(l) = l^q F_{n+1}$].

In other words, all the information can be extracted from the positive integer moments, including the value of the noninteger or of the negative moments. This makes a bridge with critical phenomena, where only a countable set of operators is considered (relevant and irrelevant). The Bernstein–Hausdorff theorem provides us with a mathematically well-defined tool to compute all the moments from the positive integer ones. This statement is physically important[7] in the case of noisy percolating

networks where there exists a probe which couples selectively to different positive integer moments, and where these positive integer moments are the only quantities observable through macroscopic noise measurements.[14] From now on, only the positive integer moments are considered in this paper. In practice, however, if other moments are needed, it may be easier to compute them directly, since the theorem applies only if the exact values of the moments are known. Nevertheless, the above result shows that the continuous dependence on q in Eq. (4) is not an insuperable difficulty to make analogies with critical phenomena. As a consequence, only the positive integer moments are considered.

4. FLUCTUATIONS OF THE MOMENTS WITH RESPECT TO THE STARTING POINT

Experimentally, one does not have a direct access to the universal function of the fixed-point equation. This implies that the origin (cubic inflection point) has to be determined numerically from the experimental data and therefore is subjected to uncertainties. In this section, we consider only the critical point. There, the rotation number ρ is irrational and the starting point of the series can be *a priori* arbitrarily chosen. One is therefore led to ask how the multifractal moments (4) are, in this case, sensitive to small variations of the starting point.

Anticipating what follows, we define the following set of functions:

$$\phi_q(F_n, x_1) \equiv M_q(F_n, x_1) / \langle\langle M_q(F_n, x_1) \rangle\rangle \tag{9}$$

with the moments M_q defined by

$$M_q(F_n, x_1) = \frac{1}{F_{n+1}} \sum_{1 \leqslant i \leqslant F_{n+1}} |\hat{f}^{(F_n)}(x_i) - x_i|^q = A_q(F_n, x_1)\, F_{n+1}^{-\tau(q)-1} \tag{10}$$

The brackets in Eq. (9) refer to an average with respect to the starting point. That type of average is discussed later in this section. In Eqs. (9) and (10), we have explicitly included the F_{n+1} dependence, which should also have appeared in the arguments of $\mathbb{P}$ in the previous section.

Figures 3a and 3b illustrate the variations of $\phi_q(F_n, x_1)$ for $q = 2$ and x_1 in the interval $[0, 1]$ for the map of Eq. (1). By increasing the time scale at which the system is probed ($n = 8$ and 11, respectively), these functions vary over the same range, but they become highly irregular objects. One concludes from these numerical results that: (i) As expected, the scaling behavior characterized by $\tau(q)$ is independent of the starting point, and (ii) In the asymptotic limit ($n \to \infty$), one has to face erratic changes of the

amplitudes $A_q(F_n, x_1)$ in Eq. (10) of the moments even for an infinitesimal shift of the starting point. To characterize the scale of the fluctuations, Fig. 4 shows the normalized root mean square, $[(\langle y^2\rangle - \langle y\rangle^2)/\langle y\rangle^2]^{1/2}$, with $y = \phi_q(F_n, x_1)$, as a function of q. Intuitively, the high-order moments are sensitive to a small part of the trajectory and therefore they are more sensitive to small variations of the starting point.

Despite the large variations in Figs. 3a and 3b, the multifractal moments (10) have invariance properties under the map when n goes to

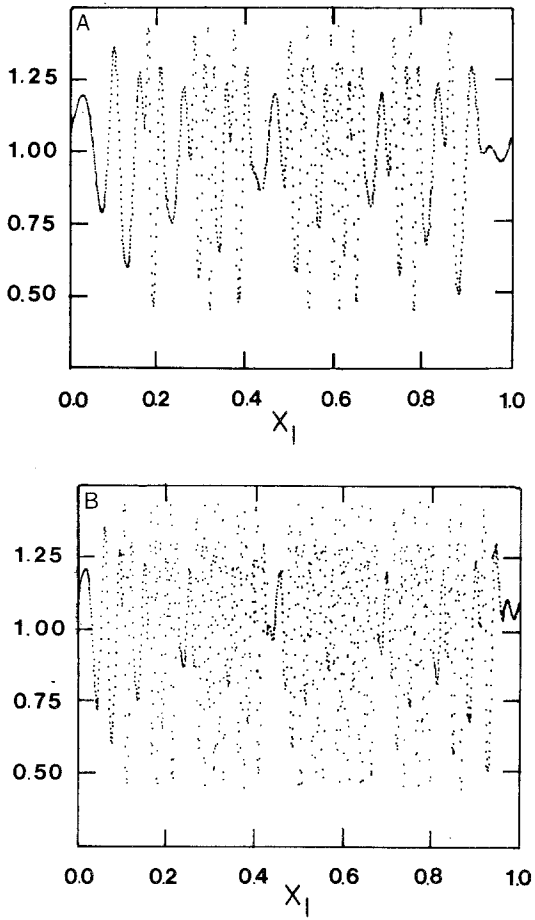

Fig. 3. Illustration of the fluctuations of the multifractal moments as a function of the starting point of the iterations. (A) Plot of the function $\phi_q(F_n, x_1)$ for $q=2$, $n=8$, as a function of x_1. (B) Plot of the function $\phi_q(F_n, x_1)$ for $q=2$, $n=11$, as a function of x_1. Note, by comparing with (A), that the range of variation of the function $\phi_q(F_n, x_1)$ is roughly the same as in the case $n=8$, but that the changes are more abrupt as a function of x_1.

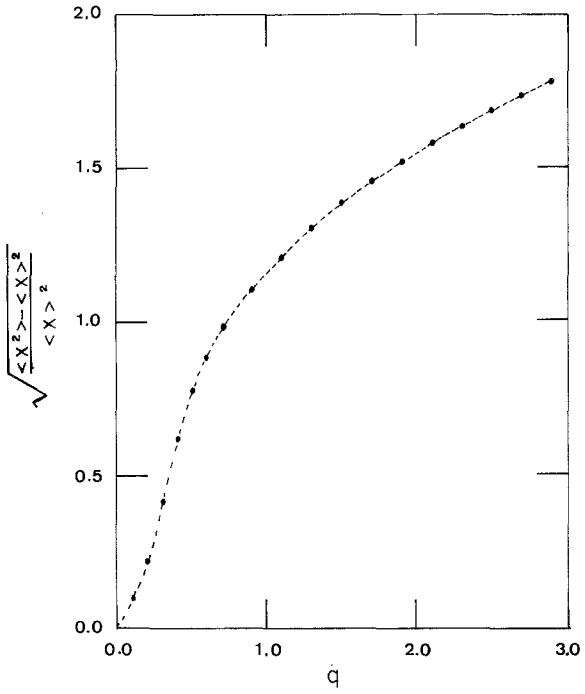

Figure 4. Variance $[(\langle y^2\rangle - \langle y\rangle^2)/\langle y\rangle^2]^{1/2}$ of the multifractal moments as a function of the order q of the moment. The average is over the starting point (taken at random with a uniform distribution) and $y \equiv M_q(F_n, x_1)$.

infinity. Indeed, let us consider their variation when the starting point is taken as $f(x_1)$ instead of x_1:

$$M_q(F_n, x_1) = M_q(F_n, f(x_1)) + \frac{1}{F_{n+1}} \{|\hat{f}^{(F_n)}(x_1) - x_1|^q - |\hat{f}^{(F_n)}(x_{F_{n+1}+1}) - x_{F_{n+1}+1}|^q\} \tag{11a}$$

From this equation, it is shown in Appendix A of the next paper that the multifractal moments are invariant under the dynamics of the map, i.e.,

$$\lim_{n \to \infty} \{M_q(F_n, x_1) = M_q(F_n, f(x_1))\} \tag{11b}$$

This can be heuristically demonstrated if one remarks that $M_q(F_n, x_1)$ differs from $M_q(F_n, f(x_1))$ by a term which goes exponentially to zero when n becomes infinity (see Appendix A of II for a more detailed discussion).

This statement holds as long as q takes finite values, since in that case the multifractal moments are not dominated by the end points of the multifractal series and the last two terms of Eq. (11a) can be discarded.

In Fig. 5, we have plotted the ratios of two multifractal moments taken at points x_1 and $f(x_1)$ as a function of the "finite size n" to illustrate numerically the invariance property (11b). On a log plot, the curve tends rapidly to a straight line, thereby corroborating that, within exponentially small corrections, the multifractal moments are invariant under the dynamics. We stress, however, that the multifractal moments normalized by their leading scaling behavior [i.e., the functions $\phi_q(F_n, x_1)$ in Eq. (9), or equivalently the amplitudes $A_q(F_n, x_1)$ in Eq. (10)] do not necessarily possess a well-defined limit for a given x_1 as n goes to infinity. And indeed, we could not numerically see signs of convergence for $n \leqslant 22$, but the variations at fixed x_1 and for different F_n do remain bounded.

From the invariance property (11b), one can show that the multifractal moments, averaged with respect to the starting point x_1, are independent of the *a priori* probability distribution with which x_1 is drawn. A more mathematical discussion of this statement can be found in Appendix A of the next paper. We did, moreover, verify numerically that the averaged multifractal moments are indeed independent of the *a priori* probability for the starting point x_1. Table I reports the results obtained for

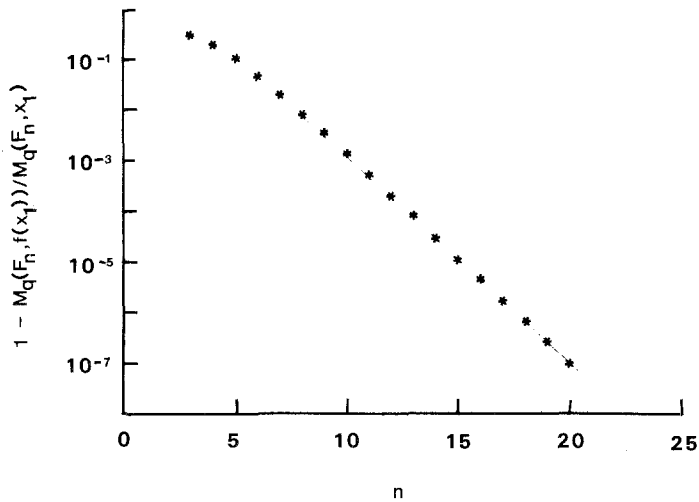

Fig. 5. Invariance [see Eq. (11b)] of the multifractal moments under the map as n goes to infinity. The curve corresponds to $1.0 - M_q(F_n, x_1)/M_q(F_n, f(x_1))$ as a function of n for $x_1 = 0.2$. As n goes to infinity, the curve tends rapidly to an exponentially decreasing function of n, thereby indicating that at the critical golden-mean winding number the multifractal moments are invariant under the map f [of Eq. (1a)].

Table I. Averaged Values of the Multifractal Moments at $K = K_c$, $\Omega = \Omega_c$, for $q = 1, 2, 3, 4$, a Coarse-Graining Scale F_8, and for Different Probability Distributions of the Starting Point

	Multifractal moments[a]				
q	(1)	(2)	(3)	(4)	(5)
1	7.21×10^{-1}	7.35×10^{-1}	7.46×10^{-1}	7.21×10^{-1}	7.23×10^{-1}
2	1.74×10^{-2}	1.76×10^{-2}	1.78×10^{-2}	1.74×10^{-2}	1.75×10^{-2}
3	7.12×10^{-4}	6.90×10^{-4}	6.73×10^{-4}	7.12×10^{-4}	7.11×10^{-4}

[a] Results (1) refer to the uniform distribution; (2) and (3) denote the values obtained when the starting point is drawn with a probability density $P(x_1) \sim x_1^{-1/\alpha}$ with $\alpha = 2$ and 3, respectively; and (4) and (5) refer to a probability distribution of the type $P(x) \sim x^{(\alpha+1)/\alpha} e^{-x^{-1/\alpha}}$, with $\alpha = 1, 2$.

different *a priori* probabilities and corroborates this invariance property within a numerical accuracy due to the relatively small value of n ($=8$) used.

As a conclusion of this section, let us remark again that the multifractal properties of maps of the circle at criticality share with critical phenomena the property of non-self-averaging. Indeed, Eq. (11b) and the fact that $\phi_q(F_n, x_1)$ is not independent of x_1 imply that for any of the $\phi_q(F_n, x_1)$, the time average of $\phi_q(F_n, x_1)$, defined as

$$\left[\sum_{i=0}^{l} \phi_q(F_n, f^{(i)}(x_1)) \right] \Big/ (l+1) \tag{12}$$

and the ensemble average {defined as the value of $\phi_q(F_n, x_1)$ averaged over x_1 in the interval $[0, 1]$}, do not coincide in the limit where l is arbitrarily large but less than F_n. Fundamentally, this comes from the existence of the correlation time discussed in Section 5.2.1: For times less than the correlation time, no self-averaging occurs and at a critical point that correlation time is infinite.

5. THE UNIVERSAL PROBABILITY DISTRIBUTIONS

At criticality, the mean rotation number is irrational, so that it does not seem natural to privilege any particular point or set of points. However, it has been shown in the preceding section that the amplitudes $A_q(F_n, x_1)$ of the multifractal moments exhibit large variations as a function of the starting point of the iteration x_1. This was summarized by the properties of the function $\phi_q(F_n, x_1)$. A natural way, then, to characterize

the curves $\phi_q(F_n, x_1)$ so that they will be useful for experiments is to treat their dependence on x_1 from a probabilistic point of view. We consider the positive integer moments of Section 2 as a set of random variables. The *a priori* probabilities that determine the statistical ensemble are those that we choose for the starting point of the iterations. We have checked numerically and demonstrated analytically (in Appendix A of II) that the choice of this *a priori* probability is to a very large extent irrelevant.

From this point of view, then, let us consider the joint probability distribution $\mathscr{P}$ for the positive integer moments. This function depends on the control parameters as well as on the time scale at which the system is probed [F_n in Eq. (10)]. Anticipating what follows, we take K, the nonlinearity parameter, and P, the period of the map, as the parameters. At criticality, P is infinite and K is set to its critical value K_c. The object of this section is to show that the following *Ansatz* is correct: $\mathscr{P}$ is a universal function, independent of the map chosen on the critical manifold, and it obeys the scaling equation

$$\begin{aligned}
&\mathscr{P}(a_0 M_0, a_1 M_1, \ldots, a_q M_q, \ldots; a_K(K-K_c), a_P P, a_P F_n) \\
&\quad = \lambda^{-\tau(0)-1}\lambda^{-\tau(1)-1}\cdots\lambda^{-\tau(q)-1} \\
&\quad \times \mathscr{P}(a_0 M_0/\lambda^{-\tau(0)-1}, a_1 M_1/\lambda^{-\tau(1)-1}, \ldots, a_q M_q/\lambda^{-\tau(q)-1}, \ldots; \\
&\qquad a_K(K-K_c)/\lambda^{-1/\nu}; a_P P/\lambda; a_P F_n/\lambda)
\end{aligned} \tag{13}$$

where the a_i are particular to the map considered. These coefficients are analogous to nonuniversal metric factors in critical phenomena.[17] These metric factors are identical for the period P and for F_n because they are both measured in the same units. Equation (13) applies to joint probability distributions of an arbitrarily large number of positive integer moments. Note that because positive integer moments suffice to characterize $\mathbb{P}$, we concentrate on those. Since the support of the M_q themselves is finite as well, we will discuss below the positive integer moments of the M_q. (The nomenclature "moments of multifractal moments" is unfortunately imposed by circumstances).

Equation (13) is the cornerstone of our approach. In other words, it contains as special cases all the universal quantities which can be measured from our point of view. It exhibits the infinite set of exponents, as well as gap scaling[18] [see Eq. (19) below] for cumulants of the variables M_q. Also, it describes not only the critical point, but also its approach through changes of either or both of the control parameters K, P, and the "finite size" parameter F_n. Finally, note that the role as well as the scaling properties of $\mathscr{P}$ are similar to those of the free energy in critical phenomena, hence the similarity in point of view.

To show the validity of Eq. (13) explicitly, and to demonstrate which of its special cases one would measure in practice, we consider various limiting cases in the following subsections, first at criticality, then in the crossover region.

5.1. At the Critical Value of the Control Parameters

A direct numerical verification of Eq. (13) in its full generality is not workable. Therefore, we first deal with partial probability distributions for one variable M_q at a time. The set of these distributions does not contain information about cross-correlations. This is studied by means of universal ratios in the second part of this section.

Let us consider the question of universality. Figure 6 shows the *cumulative* probability distribution for the variable

$$\phi_q(F_n, x_1) \equiv M_q(F_n, x_1)/\langle\langle M_q(F_n, x_1)\rangle\rangle \tag{14}$$

for $q = 1, 2, 3$. The normalization factor appearing in Eq. (14) gets rid of the nonuniversal factor a_q. To characterize the scaling properties of these distributions, the system is probed at different time scales (curves A and B on each plot) by varying the Fibonacci number entering in Eq. (13). Also, the map defined in Eq. (1b) allows us to test the hypothesis of universality (curve C on each plot). For a given value of q, the curves have been shifted for clarity, but they are actually identical on the scale of the figures. The conclusions which follow are generalizable to any value of q:

(i) The fluctuations of the normalized variables ϕ_q are independent of the time scale. In other words, there is no self-averaging for the moments defined by Eq. (14) or Eq. (10), even when n tends to infinity. This is the analog of the critical fluctuations at a continuous phase transition.

(ii) The fluctuations are independent of the chosen map on the critical manifold (maps which belong to the same universality class).

Having verified directly the scaling properties of Eq. (13) for one variable at a time, let us consider more general quantities which allow us to verify cross-correlations as well. These quantities are universal and scale independent, and play the same role as universal amplitude ratios in critical phenomena. More specifically, we consider the following ratios for averaged *cumulants* (denoted with double brackets):

$$A(q, r; k, l) \equiv \frac{\langle\langle M_q(F_n, x_1)^k\, M_r(F_n, x_1)^l\rangle\rangle}{\langle\langle M_q(F_n, x_1)\rangle\rangle^k\, \langle\langle M_r(F_n, x_1)\rangle\rangle^l} \tag{15}$$

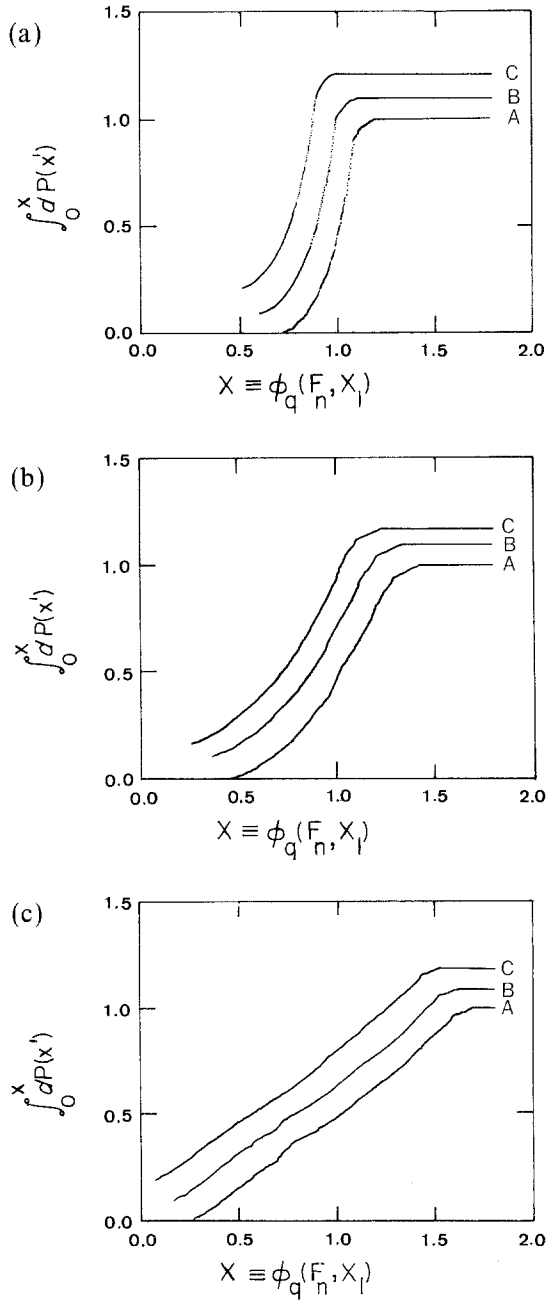

Fig. 6. Critical point universality of the cumulative probability distributions for various $x \equiv \phi_q(F_n, x_1)$, for $q = (a)$ 1, (b) 2, and (c) 3. On each plot, curves A and B correspond to Eq. (1a) with respectively $F_n = F_9$ and $F_n = F_{10}$. Curve C is for the map (1b) with $F_n = F_{12}$. The three curves on each plot are displaced vertically for clarity. The figures show that the probabilities for the multifractal moments are independent of the time scale at which the system is probed, as long as this time scale is large enough, and also show that the fluctuations are independent of the map as long as this map is on the critical manifold.

The scale independence and universality of (15) follow automatically from Eq. (13). Indeed, let us first return to the simpler case of averaged moments,

$$\langle (M_q)^k \rangle \equiv \int (M_q)^k \mathscr{P}_q(a_q M_q; F_n)\, dM_q$$

$$= a_q^{-1-k} [F_n^{-\tau(q)-1}]^k \cdots$$

$$\times \int (a_q M_q / F_n^{-\tau(q)-1})^k \mathscr{P}_q(a_q M_q / F_n^{-\tau(q)-1}; 1)$$

$$\times d[a_q M_q / F_n^{-\tau(q)-1}] \tag{16}$$

$$= a_q^{-1-k} [F_n^{-\tau(q)-1}]^k \int u^k \mathscr{P}_q(u; 1)\, du \tag{17}$$

where the limits of integration introduce only higher-order corrections to scaling, which have not been included. The integrand in Eq. (17) is a universal quantity and the particular character of the map appears only through the scale factors a_q. By taking ratios with the mean values to eliminate the a_q, one is led to

$$\frac{\langle M_q(F_n, x_1)^k\, M_r(F_n, x_1)^l \rangle}{\langle M_q(F_n, x_1) \rangle^k \langle M_r(F_n, x_1) \rangle^l} \equiv \frac{\int u^k v^l \mathscr{P}_{q,r}(u, v; 1)\, du\, dv}{[\int u \mathscr{P}_q(u; 1)\, du]^k [\int v \mathscr{P}_r(v; 1)\, dv]^l} \tag{18}$$

which is indeed a universal quantity. By generalizing to ratios of cumulants, one deduces that the $A(q, r; k, l)$ are universal quantities which also characterize the trajectory for the iterates. Table II reports numerical results when the map is either (1a) or (1b) and demonstrates that they are independent of the time scale as well as of the map. We note in passing that the cumulant averages are very sensitive to the tails of the distributions and this explains the slight statistical fluctuations of the data, especially for large order of cumulant. As mentioned earlier, we have also checked that the above results are independent of the *a priori* distribution of the starting point.

In closing this section, note that the scaling found in Eq. (17),

$$\langle (M_q)^k \rangle \approx F_{n+1}^{-k(\tau(q)+1)} \tag{19}$$

corresponds to what is known as "gap scaling" in critical phenomena.[18]

5.2. Crossover from the Critical Region

As mentioned above, to approach the critical point experimentally, one sets the mean rotation number equal to successive rational approxima-

tions of the golden mean. The following analysis characterizes the crossover between the region where fluctuations are critical and the region where they correspond to a pure rotation. The borderline between the two regimes corresponds to a unique characteristic time scale which is analogous to the correlation length in critical phenomena. The analysis is developed in the two eigendirections of the renormalization group. In Section 5.2.1 we give an operational definition of the correlation time, and in Section 5.2.2 we study specific functions and exhibit their universal crossover behavior at that characteristic time.

Table II. Universal Ratios Defined by Eq. (15)[a]

	$A(q, r; k, l)$	
$q, r; k, l$	I	II
1020	0.0100(2)	0.0101(2)
1030	$-7.2(1)10^{-4}$	$-7.0(2)10^{-4}$
0202	0.0521(4)	0.0525(9)
0203	−0.0051(2)	−0.0051(1)
0204	−0.0017(1)	−0.0019(1)
1211	0.0187(2)	0.0192(2)
1221	−0.00117(5)	0.00119(4)
1212	−0.00227(5)	−0.00235(5)
0302	0.172(1)	0.166(4)
0303	−0.0075(5)	−0.0074(5)
0304	−0.036(1)	−0.033(1)
1311	0.0226(8)	0.0246(8)
1321	0.0015(1)	0.0015(1)
1312	−0.0037(2)	0.0033(2)
0402	0.363(1)	0.363(1)
0403	0.0262(5)	0.0262(6)
0404	−0.186(3)	−0.186(5)
1411	0.0236(5)	0.0236(5)
1412	−0.0320(5)	−0.0320(8)
2311	0.0867(7)	0.0870(9)
2312	−0.0076(5)	−0.0076(2)
2321	−0.0064(5)	−0.0065(5)
2411	0.114(5)	0.114(6)
2412	−0.0036(5)	−0.027(5)
2421	−0.0063(5)	−0.0063(3)
3411	0.244(1)	0.244(1)

[a] Column I is for the map defined by (1a) and column II for the map (1b). The results are for F_{10} and 2×10^4 samples. The ratios computed for larger F_n (we have checked $n = 10$–12) or for the above two maps are within the statistical uncertainty on the last digit (written in parentheses).

5.2.1. Definition of the Characteristic Time

On the Discontinuity Line. On the discontinuity line, ρ is irrational. The map is not a pure rotation, but both problems are in fact topologically conjugate through a change of coordinates. The existence of the conjugacy in the subcritical region has been proven by Denjoy for maps with bounded variations (see ref. 13). The extension of this result to the critical line is due to Yoccoz.[19] In other words, the result of these works is that there exists a function h such that

$$f \circ h = h \circ R_\sigma \Leftrightarrow f = h \circ R_\sigma \circ h^{-1} \tag{20}$$

where the pure rotation R_σ is defined by

$$R_\sigma(x) = x + \sigma \tag{21}$$

The key point is that this conjugacy to a pure rotation is differentiable everywhere but at the critical point.

The intuitive definition of the characteristic time is the time (number of iterations) over which the iterates must be averaged before they appear to behave as if they were the iterates of a pure rotation. In the case where h is differentiable, the closest-return distances for f are asymptotically proportional to those of R_σ. Indeed, the closest-return distances of R_σ for F_n iterations are $\sigma F_n - F_{n-1} = -(-\sigma)^n$, while for f, using Eq. (21),

$$\begin{aligned} \hat{f}^{(F_n)}(x) - x &= h \circ \hat{R}_\sigma^{(F_n)} \circ h^{-1}(x) - x \\ &= h \circ [h^{-1}(x) - (-\sigma)^n] - x \\ &\cong -(-\sigma)^n \left. \frac{dh(y)}{dy} \right|_{y = h^{-1}(x)}, \qquad n \gg 1 \end{aligned} \tag{22}$$

Heuristically, the fluctuations of the moments of the closest-return distances (multifractal moments) disappear in the long-time limit where approximation (22) holds. This can be seen by substituting (22) in the sum (10) defining the multifractal moments and noting that the only dependence on iterates is through the derivative of the homeomorphism; since this is a smooth function of x, this x dependence is self-averaging on an irrational trajectory. One concludes that, below the critical line, the fluctuations of the moments with respect to the starting point vanish in the infinite-n limit. (The relationship between the multifractal moments and the conjugate. homeomorphism is discussed further in the next paper.)

To characterize the time scale on which these fluctuations disappear, let us first define a set of "times" by the relation

$$\xi_q \equiv \sum_{k \geqslant 1} F_k [\langle\langle \phi_q(F_k, x_1)^2 \rangle\rangle / \langle\langle \phi_q(F_k, x_1) \rangle\rangle^2] \tag{23}$$

Again the cumulant averages are taken over the starting point of the iterations. This is analogous to the definition of a correlation length for thermodynamic systems. We show below that this quantity is worth defining because all the q dependence can be put into a prefactor, while the scaling behavior can be described by a q-independent exponent.

When the map is a pure rotation ($K=0$), all the ξ_q are identically equal to zero. As the K parameter is increased along the discontinuity line, the fluctuations are more and more important and the ξ_q diverge at criticality. Figure 7a demonstrates on a log-log plot that this divergence is characterized by a *unique* exponent, irrespective of the value of q. Thus, one defines a unique *characteristic time* ξ as

$$\xi_q \equiv C_q \xi, \qquad \forall q \tag{24}$$

where C_q is a bounded function of q. It is found numerically that ξ diverges near criticality as

$$\xi \equiv (1 - K/K_c)^{-\nu} \tag{25}$$

with $\nu \cong 1.00$, in good agreement with the renormalization group result[2] $\nu \cong 0.996...$.

On the Critical Line. In the other unstable direction of the renormalization group, $K=1$, one considers periodic orbits of period $P = F_{n+1}$. One can show that the set of arcs drawn between x_i and $\hat{f}^{(F_n)}(x_i)$ cover the whole circle without overlap. Once the parameters K and Ω are chosen, the stable orbit is perfectly defined and the moments in Eq. (4) do not depend on the starting point, as long as it is chosen on this orbit. However, the system is in a phase-locking interval with a given mean rotation number (i.e., a given periodicity $P = F_{n+1}$) for an open interval of Ω. Since we take P instead of Ω as a variable in Eq. (13), it is natural to average the moments over the orbits corresponding to the different values of Ω for which the stable orbits of period $P = F_{n+1}$ exist. The definition equivalent to Eq. (23) is

$$\xi_q \equiv \sum_{k \geqslant 1}^{k=n+1} F_k [\langle\langle \phi_q(F_k, x_1)^2 \rangle\rangle / \langle\langle \phi_q(F_k, x_1) \rangle\rangle^2] \tag{26}$$

where this time the average is over all possible orbits consistent with a given period (for each term, $P = F_{k+1}$). In that case, the only characteristic time is proportional to the period. Figure 7b demonstrates that all the ξ_q are indeed proportional to P and this defines again a unique characteristic time through

$$\xi_q = B_q P \tag{27}$$

where B_q has a smooth variation with respect to q.

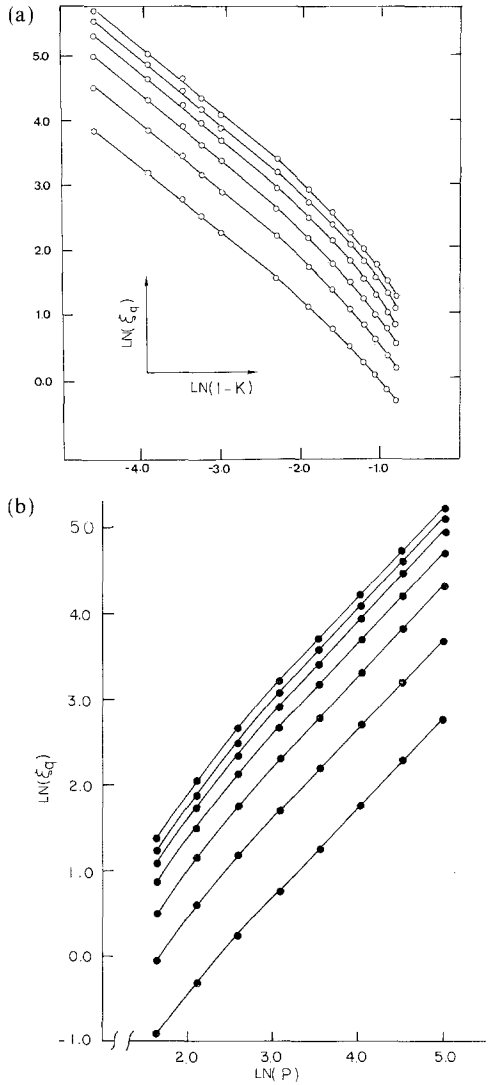

Fig. 7. Scaling of the characteristic time ξ. (a) Log-log plot of the function ξ_q defined by Eq. (23) as a function of $(1-K)$ for various values of q. The lower curve is for $q=2$, with q increasing up to the uppermost curve $q=7$. The map considered is (1a) when the critical point is approached along the discontinuity line where the mean winding number is equal to the golden mean. The curves become straight lines as K tends to its critical value $K_c=1$, and the slope is independent of the order q of the moment. (b) Log-log plot of the function ξ_q defined by Eq. (26) as a function of the period of the orbit when the critical point is approached by changing the period P of orbits of length F_n along the critical line $K=1$. For large values of P, the curves become a straight line whose slope is independent of q ($q=1$–7 as one moves from the lowest to the highest curve).

To conclude this section, one remarks that definitions (23) and (26) are equivalent. Indeed, when one changes Ω on a locking interval, a given stable point of the orbit changes continuously. Hence, averaging over Ω is like averaging over starting points. In the latter case, one must make sure that, for a given starting point, Ω is chosen so that this point belongs to a stable orbit. Since the statistical results are independent of the *a priori* distribution, averaging over locking intervals or over starting points gives the same results. At an irrational winding number (on the discontinuity line), however, the interval over which Ω can vary reduces to a single point, and there is an infinity of equivalent starting points. In both eigendirections, then, the *a priori* probabilities are in a sense given by a random choice of starting point. Furthermore, the period P is equal to F_∞ on the discontinuity line, so that Eq. (26) does reduce to Eq. (23).

In the general case, i.e., not along a particular eigendirection, Eq. (13) suggests that the characteristic time (correlation length) obeys the following scaling law:

$$\xi = P\mathscr{F}(C_\xi(1 - K/K_c)/P^{-1/\nu}) \tag{28}$$

where $\mathscr{F}$ is a universal crossover function, with C_ξ a nonuniversal scale factor.

5.2.2. Crossover Behavior. When the system is probed at shorter scales than the scale ξ defined above, the fluctuations are of the same order as in the critical regime. On the other hand, if the system is probed at scales larger than ξ, the map is in fact equivalent to a pure rotation and the fluctuations disappear. The time scale over which the fluctuations are probed is given by the variable F_n appearing in Eq. (13). This is the same F_n as the one appearing in Eqs. (9) and (10), for example. It plays a role analogous to inverse wave vector or finite size in critical phenomena. The relative role of F_n and of the caracteristic time ξ is dramatically illustrated in Fig. 8, where F_n is varied so that the cumulative distribution for one of the moments crosses over from a critical-type behavior ($F_n/\xi \ll 1$) to the step function corresponding to the pure rotation case ($F_n/\xi \gg 1$).

In the general case, the averaged multifractal moments are described by crossover functions which depend on the control parameters K and P as well as on the time scale at which the system is probed F_n [see Eq. (10)]. As in Eq. (13), in the case of periodic orbits, this "finite-size" time scale is not necessarily related to the period. A consequence of Eq. (13) is that the multifractal moments behave as

$$\langle M_q(K - K_c, P, F_n)\rangle \equiv \lambda^{-\tau(q)-1}\mathscr{G}_q(a_K(1 - K/K_c)/\lambda^{-1/\nu}, a_P P/\lambda, a_P F_n/\lambda) \tag{29}$$

where, up to an overall factor, the function $\mathscr{G}_q$ is a universal function, but where a_K and a_P are particular to the map. While (29) also applies without the need to average when the starting point is the origin, we present the results mainly for the averaged case, which we believe is also more relevant experimentally. We first check (29) on the critical line where the map is locked with a period corresponding to the Fibonacci numbers.

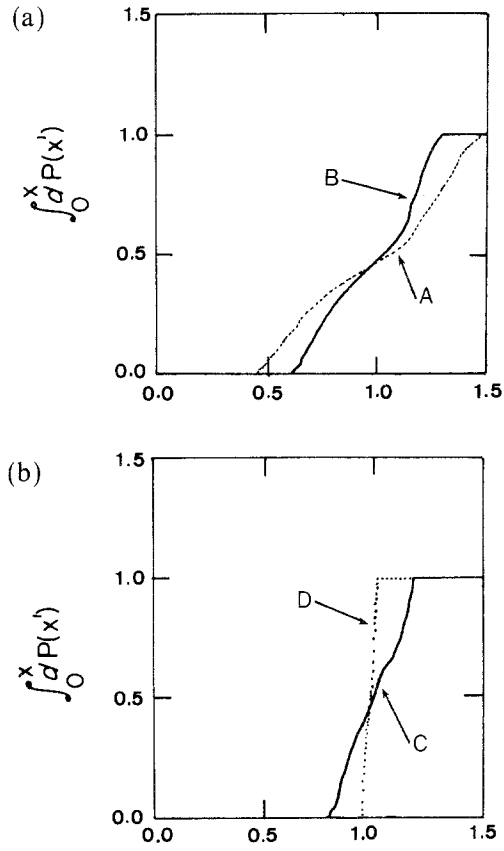

Fig. 8. Crossover of the cumulative probability distribution for the normalized moment $\phi_q(F_n, x_1)$, for $q=3$, as the coarsening time F_n is changed. The map is (1a) with $K=0.97$ and $\Omega(K)$ chosen so that we are on the discontinuity line where the mean rotation number is the golden mean (approximated here by F_{27}/F_{28}). Curve A is for $n=8$, curve B for $n=9$, curve C for $n=10$, curve and D for $n=11$. Let ξ be the characteristic time defined by Eq. (23). Since $F_7/\xi \ll 1$, curve A is similar to the critical point plots of Fig. 6, and since $F_{11}/\xi \gg 1$, the last curve D is like that for a pure rotation, where all distances entering the multifractal moments are identical and independent of the starting point. Under coarsening of the time scale F_n, one crosses over from critical fixed-point to trivial fixed-point behavior.

On the Critical Line $K=K_c=1$ and $P=F_{n+1}$. Equation (29) predicts that the moments of the closest-return distances scale as $P^{-\tau(q)-1}$. Table III reports some numerical results for the superstable orbits. One notes in passing that this is an efficient algorithm to compute the set of $\tau(q)$ in the large-q limit. We have checked that Eq. (29) also holds when the "finite-size" time scale is any of the Fibonacci numbers F_k such that $F_k < F_{n+1}$ ($\equiv P$).

For $K\neq 1$ and $P=F_{n+1}$. Eq. (29) implies that

$$\langle M_q(K-K_c, P, F_n)\rangle \equiv (a_P P)^{-\tau(q)-1}\mathcal{G}_q(b(1-K/K_c)/P^{-1/\nu}, 1, \sigma) \quad (30)$$

where $b=a_K/a_P^{-1/\nu}$. Figure 9 verifies, for $q=3$, the scaling prediction (30) that, for different $F_n=\sigma P$ and $(1-K/K_c)$, all points collapse on a single function $\mathcal{G}_q$. Apart from the usual metric factors, the crossover scaling function is also universal, as can be checked in Fig. 9 by the fact that on a log-log plot the scaling functions for two different maps are identical within a shift of the origin. In the limit K goes to K_c, we recover in Fig. 9 that the multifractal moment scales as $P^{-\tau(q)-1}$. On the other hand, as P tends to infinity with $F_n/P=\sigma$ and K fixed, one goes to a pure rotation as soon as F_n is larger than ξ. In that limit, the multifractal moment scales trivially as P^{-q}, which, through $\mathcal{G}_q(y)=y^{\nu(\tau(q)+1-q)}$, implies the straight line of slope -0.5 in Fig. 9.

Scaling relations such as (29) or (30), which hold for averaged multifractal moments, or for multifractal moments of superstable orbits, should be accessible experimentally. The study of crossover presented here is a

Table III. Numerical Values of the Exponent $\tau(q)$[a]

	$\tau(q)$		
q	I	II	III
1	0.00	0.00	0.00
2	0.83	0.84	0.81
3	1.49	1.52	1.48
4	2.07	2.10	2.07
5	2.61	2.64	2.62

[a] Calculated (1) at the critical point, using Eq. (4); (2) on superstable periodic orbits located on the $K=K_c$ line using Eq. (29) and $P=F_{n+1}$ for $6\leqslant n\leqslant 13$; and (3) using the analytic results obtained from the linear approximation (paper II).

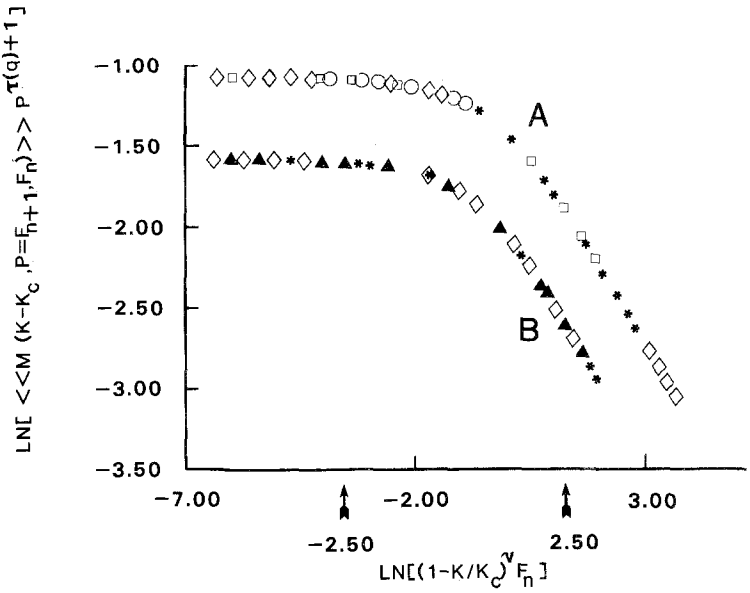

Fig. 9. Universal crossover functions for the averaged multifractal moments $\langle\langle M_q(K-K_c, P=F_{n+1}, F_n)\rangle\rangle$. The quantity $\ln[\langle\langle M_q(K-K_c, P=F_{n+1}, F_n)\rangle\rangle P^{\tau(q)+1}]$ is plotted versus $\ln[(1-K/K_c)^{\nu} F_n]$ for $q=3$. For curve A, the map is that of Eq. (1a) with $K_c=1$ and for values of $P=F_{n+1}$ between F_{14} and F_{18} with $2\times10^{-7}<(K_c-K)<10^{-2}$. The different symbols correspond to different values of n and K. Averages are taken over 1000 starting points. All the points fall on a single curve, confirming the existence of the scaling function (30). For curve B, the map is that of Eq. (1b). The horizontal scale is shifted slightly, as indicated by the arrows. In this case, $K_c=0.625$ and n is chosen as $n=17, 18, 19$. Note that curves A and B coincide with each other by a shift of the origin. This shows that the scaling function is universal aside from the nonuniversal constants b, and $a_P^{-\tau(q)-1}$ times the scale factor of $\mathscr{G}_q$. [See Eq. (30).]

more general alternative to the analysis of Arneodo and Holschneider,[20] since it identifies the diverging reference time ξ, takes into account both eigendirections, and proceeds through universal crossover functions instead of parameter-dependent exponents.

6. CONCLUSION

The object of this paper was to point out that the multifractal properties of maps of the circle can be basically cast in the language of critical phenomena. In this conclusion, we discuss our results in connection with other work and suggest extensions.

At criticality, the fluctuations of the moments of the closest-return distances (multifractal moments) as a function of the starting point of the

iteration have been shown to be universal in the renormalization group sense: They are scale independent and are a universal characteristic of all the maps on the critical manifold. Multifractal properties of maps of the circle which are a direct consequence of the functional renormalization group of Rand *et al.* (see next paper) are thus characterized in the multifractal approach not only by an infinite set of exponents, but also by an infinite hierarchy of universal ratios. The analogous quantities are known to be universal in critical phenomena. Here they provide a convenient additional way to access experimentally the universal properties of the trajectories. All of the above properties are summarized in Eq. (13) by a joint probability distribution for the positive integer moments (integer q) which contains the information about the multifractal structure of the trajectory. This joint probability distribution is independent of the *a priori* probability for the starting point, is universal, and clearly exhibits the infinite set of exponents, as well as the parameters which control the characteristic time ξ, Eqs. (23) and (26), and the quantities which obey gap scaling [Eq. (19)].

Even without the model provided by critical phenomena, the probabilistic approach suggests itself naturally because of the strong dependence of the amplitude of multifractal moments on the starting point. In the usual approach, one always takes the inflection point of the map as the starting point. Although this approach is conceptually valid, one has to consider the practical problem of determining this point in experiments with an accuracy which becomes arbitrarily large at the critical point. Whereas the value of the exponents does not depend on the starting point, there is further universal information contained in the dependence of the amplitudes of the multifractal moments on the starting point, but it is not practical to try to determine this dependence, illustrated in Fig. 3. Curves such as these are indisputably better characterized by their statistical properties. Besides the lack of self-averaging of the multifractal moments at the critical point, the functions $\phi_q(F_n, x_1)$ of Fig. 3 have no limit as n goes to infinity. Taking the averaged multifractal ratios is a statistical way to bypass these difficulties while retaining universal information which is shown in II to be related to the spectrum.

Very irregular variations are generic of a pointwise characterization of the scaling structure. For example, Feigenbaum's scaling function[21] has a rich self-similar structure. Experimentally,[3] the envelope of this function seems accessible, but the above point of view could add to the multifractal approach a test of other universal properties (amplitude ratios) of the scaling structure which, we contend, would be much easier to carry through with great accuracy than a measurement of Feigenbaum's scaling function.

In the crossover region, the averaging is over phase-locking intervals

in the case of periodic orbits and over starting points of the iterations in the case of irrational orbits. The latter procedure is in fact a limiting case of the first one. Averaging over phase-locking intervals could probably be extended to averaging over intervals of fixed period in the case of the period-doubling route to chaos. In the present case, it has been shown that, as in critical phenomena, there exists in the crossover region a unique characteristic time, which can be defined within the multifractal framework, and which marks the borderline of the critical region. As in critical phenomena, this time scale is concomitant with the concept of universality. The study presented in the last section is a more general alternative to the analysis of Arneodo and Holschneider,[20] who characterized the crossover by a Taylor expansion of the critical exponents with respect to one control parameter along one eigendirection. Crossover functions are more usual than parameter-dependent exponents (crossover functions also appear in the characterization of locking intervals; see, e.g., ref. 22). The present paper, moreover, showed that the set of $\tau(q)$ is accessible in the neighborhood of criticality by techniques which are standard in the finite-size scaling analysis of critical points [Eq. (29) and Table III]. Some of the applications of the present approach to the case of period doubling have been verified, but none of the results are presented in the present paper. We would like to encourage other researchers to purse that line of inquiry.

APPENDIX

Even though the $f(\alpha)$ function does not play a special role in our approach, we would like to introduce this function in a way which is equivalent to the traditional one,[5] but which is more natural within our approach. This is a transposition of the results of ref. 23. It suffices to remark that from the definitions of Eqs. (6), (4), and (10) we have

$$M_q(F_n, x_1) = A_q(F_n, x_1)\, F_{n+1}^{-\tau(q)-1} = \int_0^1 dl\, l^q \mathbb{P}(x_1, l, F_{n+1}) \tag{A1}$$

By a change of variables and with the definition

$$\mathbb{P}(x_1, l, F_{n+1})\, dl \equiv \hat{\mathbb{P}}(x_1, -\ln l, F_{n+1})\, d(-\ln l)$$

we obtain

$$A_q(F_n, x_1)\, F_{n+1}^{-\tau(q)-1} = \int_0^\infty d(-\ln l) \exp[-q(-\ln l)]\, \tilde{\mathbb{P}}(x_1, -\ln l, F_{n+1}) \tag{A2}$$

The multifractal moments are thus the Laplace transform of the probability $\tilde{\mathbb{P}}$. Using the Bromwich inversion formula for the Laplace transform, one can invert Eq. (A2) to obtain the scaling properties of $\tilde{\mathbb{P}}$ itself. To simplify the notations, we denote the function $A_q(F_n, x_1)$ as A_q. We have

$$\begin{aligned}\tilde{\mathbb{P}}(x_1, -\ln l, F_{n+1}) &= \int_{\varepsilon - i\infty}^{\varepsilon + i\infty} \frac{dq}{2\pi i} A_q F_{n+1}^{-\tau(q)-1} e^{q(-\ln l)} \\ &= F_{n+1}^{-1} \int_{\varepsilon - i\infty}^{\varepsilon + i\infty} \frac{dq}{2\pi i} \exp\left[\ln F_{n+1}(-\tau(q) + q\frac{-\ln l}{\ln F_{n+1}} + \frac{\ln A_q}{\ln F_{n+1}}\right] \end{aligned} \tag{A3}$$

where $i^2 = -1$. From its definition as a Laplace transform in Eq. (A2), $-\tau(q)$ is an analytic function of q for $\mathrm{Re}(q) > 0$. General theorems on the convexity of the logarithm of the moments of a probability distribution[15] tell us that $\ln[A_q F_{n+1}^{-\tau(q)-1}]$ is a convex function of q. However, in the limit $n \to \infty$, since A_q is a bounded and smoothly varying function of q (see Fig. 4), this means that the function $-\tau(q)$ itself is convex and non-increasing. In the same limit, $\ln A_q / \ln F_{n+1}$ can be neglected in (A3). In the limit $\alpha = -\ln l / \ln F_{n+1}$ finite, $\ln F_{n+1}$ infinite, one then deforms the contour to obtain, in the saddle point approximation,

$$\tilde{\mathbb{P}}(x_1, \alpha, F_{n+1}) = C(x_1, \alpha, \ln F_{n+1})\, F_{n+1}^{-1} F_{n+1}^{f(\alpha)} \tag{A4}$$

where $C(x_1, \alpha, \ln F_{n+1})$ depends weakly on $\ln F_{n+1}$ and $f(\alpha)$ is the Legendre transform of $-\tau(q)$, i.e., $\partial\tau(q)/\partial q = \alpha$; $f(\alpha) = q\alpha - \tau(q)$. Let us note in passing that the result (A4) holds only in the limit where the *logarithm* of the time scale F_{n+1} is large, whereas the usual asymptotic limit in critical phenomena, or here for the asymptotic form (4) of the multifractal moments, is obtained when the time scale itself is large. Hence in practice, the scaling regime where Eq. (A4) can be directly measured is difficult to attain. Note that a method to compute the function $f(\alpha)$ without Legendre transforming $\tau(q)$ has been recently proposed by Chhabra and Jensen.[24] Although their method allows one to get rid of the smoothing procedure for the experimental data, it cannot overcome the intrinsic difficulty of being in the regime where not only the time scale, but also its *logarithm* are large.

ACKNOWLEDGMENTS

We are especially indebted to J. Sethna, for sharing his insights on the circle map and for discussions and suggestions, and to J. Bélair, for sugges-

tions and for a thorough critical reading of an early version of this work. We would also like to thank E. Siggia for useful discussions. B. F. would like to acknowledge M. Wortis for useful discussions concerning the presentation of this paper. We are grateful for the hospitality of Cornell University, where this work was undertaken. Support there was provided by the NSF under grant DMR-85-166-16 administered by the Cornell University Materials Science Center. B. F. was supported by the Centre de Recherche en Physique du Solide (Fonds pour la Formation des Chercheurs et l'Aide à la Recherche, Québec). A.-M.S.T. is supported by the Natural Sciences and Engineering Research Council of Canada, and by the Steacie Foundation.

REFERENCES

1. J. Stavans, F. Heslot, and A. Libchaber, *Phys. Rev. Lett.* **55**:596 (1985); M. H. Jensen, L. P. Kadanoff, A. Libchaber, I. Procaccia, and J. Stavans, *Phys. Rev. Lett.* **55**:2798 (1985); J. A. Glazier, G. Gunaratne, and A. Libchaber, *Phys. Rev. A* **37**:537 (1988); J. Stavans, *Phys. Rev. A* **35**:4314 (1987); E. G. Gwinn and R. M. Westervelt, *Phys. Rev. Lett.* **59**:157 (1987); Z. Su, R. W. Rollins, and E. R. Hunt, *Phys. Rev. A* **36**:3515 (1987).
2. S. J. Shenker, *Physica* (Amsterdam) **5D**:405 (1982); M. J. Feigenbaum, L. P. Kadanoff, and S. J. Shenker, *Physica* (Amsterdam) **5D**:370 (1985); D. Rand, S. Ostlund, J. P. Sethna, and E. D. Siggia, *Phys. Rev. Lett.* **49**:132 (1985); S. Ostlund, D. Rand, J. P. Sethna, and E. D. Siggia, *Physica* (Amsterdam) **8D**:303 (1983).
3. A. L. Belmonte, M. J. Vinson, J. A. Glazier, G. H. Gunaratne, and B. G. Kenny, *Phys. Rev. Lett.* **61**:539 (1988).
4. A. Aharony, R. J. Birgeneau, J. D. Brook, and J. D. Lister, *Phys. Rev. Lett.* **57**:1012 (1986); J. D. Brook, A. Aharony, R. J. Birgeneau, E. W. Evanslutterodt, J. D. Lister, P. M. Horn, G. B. Stephenson, and A. R. Tajbakhsh, *Phys. Rev. Lett.* **57**:98 (1986).
5. T. C. Halsey, M. H. Jensen, L. P. Kadanoff, I. Procaccia, and B. I. Shraiman, *Phys. Rev. A* **33**:1141 (1986), **34**:1601 (1986); U. Frish and G. Parisi, in *Turbulence and Predictability of Geophysical Flows and Climate Dynamics* (Proceedings of the International School of Physics "Enrico Fermi," Cours LXXXVIII, Varenna, 1983), N. Ghil, R. Benzi, and G. Parisi, eds. (North-Holland, Amsterdam, 1985), p. 84.
6. G. Paladin and A. Vulpiani, *Phys. Rep.* **156** (1987).
7. B. Fourcade, P. Breton, and A.-M. S. Tremblay, *Phys. Rev. B* **36**:8925 (1987); A.-M. S. Tremblay and B. Fourcade, in *Universalities in Condensed Matter*, R. Jullien, L. Peliti, R. Rammal, and N. Boccara, eds., (Springer, Berlin, 1988).
8. B. Fourcade and A.-M. S. Tremblay, *Phys. Rev. Lett.* **64**:2659 (1990).
9. B. Fourcade and A.-M. S. Tremblay, in *Universalities in Condensed Matter*, R. Jullien, L. Peliti, R. Rammal, and N. Boccara, eds. (Springer, Berlin, 1988); see also B. Fourcade, Ph.D. thesis, Université de Sherbrooke (1988), unpublished.
10. L. P. Kadanoff, *J. Stat. Phys.* **43**:395 (1986).
11. P. Bergé, Y. Pomeau, and C. Vidal, *Order within Chaos* (Hermann, Paris, and Wiley, New York, 1984).
12. M. H. Jensen, P. Bak, and T. Bohr, *Phys. Rev. A* **30**:1960, 1970 (1984).
13. M. R. Hermann, Sur les Conjugaisons différentiables des difféomorphismes du Cercle à des Rotations, *Publ. IEHS* **49**:5 (1979).

14. R. Rammal, C. Tannous, and A.-M. S. Tremblay, *Phys. Rev. A* **31**:2662 (1985); *Phys. Rev. Lett.* **54**:1718 (1985); see also L. De Arcangelis, S. Redner, and A. Coniglio, *Phys. Rev. B* **31**:4725 (1981).
15. W. Feller, *An Introduction to Probability Theory and Its Applications* (Wiley, New York, 1971).
16. I. P. Cornfeld, S. Y. Fomin, and Ya. G. Sinai, *Ergodic Theory* (Springer Verlag, 1982).
17. V. Privman and M. E. Fisher, *Phys. Rev. B.* **30**:322 (1984).
18. M. E. Fisher, in *Scaling, Universality and Renormalisation Group Theory*, (Springer-Verlag, Heidelberg, 1983).
19. J. C. Yoccoz, *C. R. Acad. Sci. Paris* **298** (1984).
20. A. Arneodo and M. Holschneider, *Phys. Rev. Lett.* **58**:2007 (1987).
21. M. J. Feigenbaum, *J. Stat. Phys.* **19**:25 (1978), **21**:669 (1979); *Physica* (Amsterdam) **7D**:16 (1983).
22. P. Alstrøm, L. K. Hansen, and D. R. Rasmussen, *Phys. Rev. A* **36**:827 (1987).
23. B. Fourcade and A.-M. S. Tremblay, *Phys. Rev. A* **36**:2352 (1987).
24. A. Chhabra and R. V. Jensen, *Phys. Rev. Lett.* **62**:1327 (1989).